Title
Probabilistic impact of electricity tariffs on distribution grids considering adoption of solar and storage technologies

Authors
Heleno, Miguel
Sehloff, David
Coelho, Antonio
et al.

Publication Date
2020-12-01

DOI
10.1016/j.apenergy.2020.115826

Peer reviewed

LBNL-0000

Lawrence Berkeley National Laboratory

Probabilistic Impact of Electricity Tariffs on Distribution Grids Considering Adoption of Solar and Storage Technologies

M. Heleno[a], D. Sehloff[b], A. Coelho[c], A. Valenzuela[a].

a Lawrence Berkeley National Lab, 1 Cyclotron Rd, Berkeley, CA 94720
[b] University of Wisconsin, Madison, WI, USA
[c] INESC TEC, Porto, Portugal

Published in Applied Energy

December 2020

Partial funding for this work was provided by the Office of Electricity, Microgrids R&D and Advanced Grid Modeling Programs, of the U.S. Department of Energy under Contract No. DE-AC02-05CH11231.

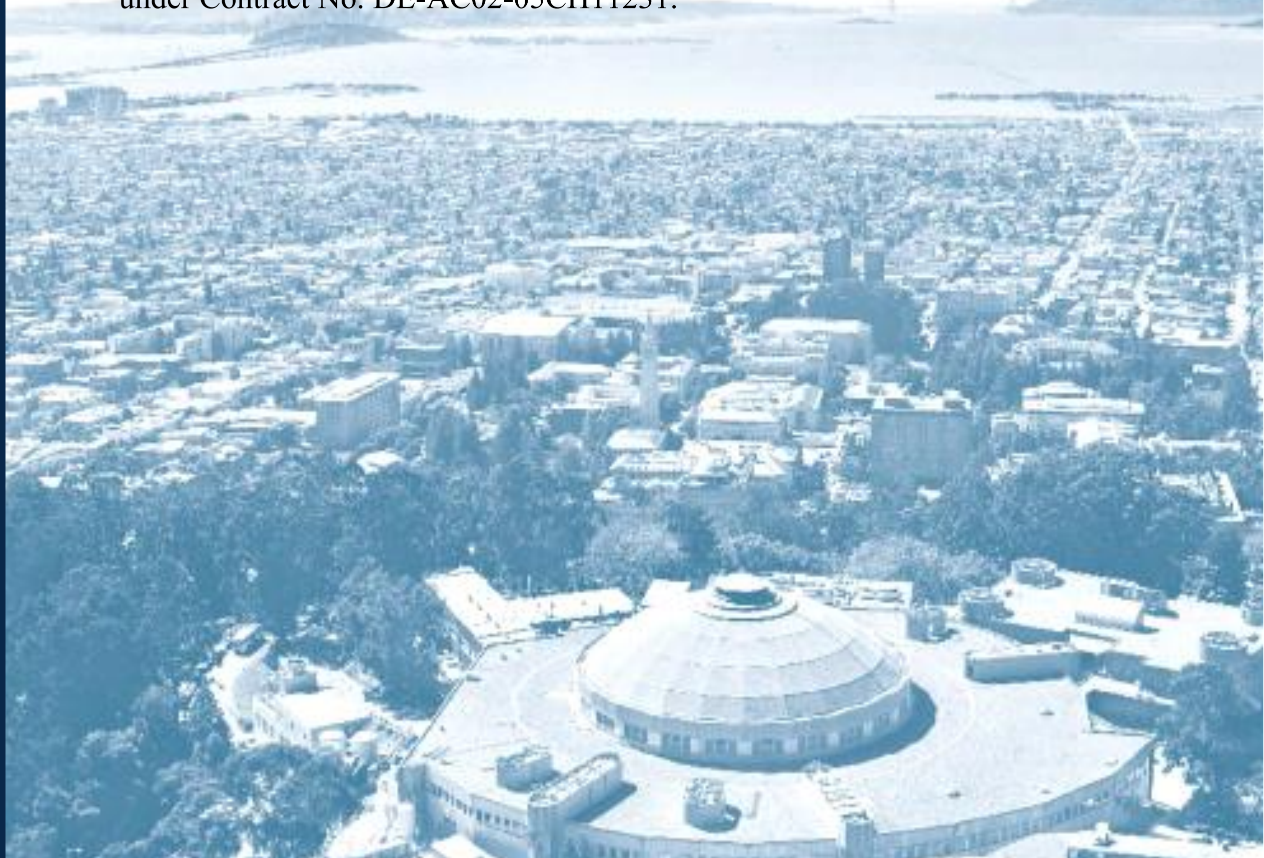

Disclaimer

Probabilistic Impact of Electricity Tariffs on Distribution Grids Considering Adoption of Solar and Storage Technologies

Miguel Heleno[a,*], David Sehloff[b], Antonio Coelho[c], Alan Valenzuela[a]

[a] *Lawrence Berkeley National Laboratory, Berkeley, CA, USA*
[b] *University of Wisconsin, Madison, WI, USA*
[c] *INESC TEC, Porto, Portugal*

Abstract

This paper models the role of electricity tariffs on the long-term adoption of photovoltaic and storage technologies as well as the consequent impact on the distribution grid. An adoption model that captures the economic rationality of tariff-driven investments and considers the stochastic nature of individual consumers' decisions is proposed. This model is then combined with a probabilistic load flow to evaluate the long-term impacts of the adoption on the voltage profiles of the distribution grid. To illustrate the methodology, different components of the electricity tariffs, including solar compensation mechanisms and time differentiation of Time-of-Use (ToU) rates, are evaluated, using a case study involving a section of a medium-voltage network with 118 nodes.

Keywords: Rate Design, Distributed Energy Resources, Distribution Grid Planning, Probabilistic Load Flow.

Nomenclature

Sets

$\mathcal{T}_{yr}$ Set of hourly time points over a year, indexed by t

$\mathcal{N}$ Set of nodes in the network, indexed by n

$\mathbb{C}$ Set of prototypical consumers, indexed by c

$\mathbb{C}_R$ Subset of prototypical residential consumers

$\mathbb{C}_S$ Subset of prototypical services consumers

$\mathbb{U}$ Set of actual consumers, indexed by u

$\mathcal{I}_t$ Set of consumers connected to utility at time t

*Corresponding author
Email address: miguelheleno@lbl.gov (Miguel Heleno)

$\mathbb{K}$ Set of technology types (PV, Storage), indexed by k or by technology type {pv,s}

Parameters

$\overline{LC_{c,t}}$ Normalized prototypical load of consumer type c at time t

$L_{n,t}$ Load of node n at time t (kW)

LC_t Load of a prototypical consumer at time t (kW)

SR_n Ratio between services and residential power at node n

E_{sr} Admissible disaggregation error in services/residential load

PR_c Reference power for prototypical consumer c

E_{pr} Admissible disaggregation error in reference power for prototypical consumers

$CFix_k$ Fixed cost of technology k (\$)

$CVar_k$ Variable cost of technology k (\$/kW or \$/kWh)

Ann_k Ann. interest rate for investments in tech. k

EC_t Energy cost at time t (\$)

FI_t Feed-in remuneration at time t (\$)

$CEff$ Charging efficiency of the battery

$DEff$ Discharging efficiency of the battery

PCr Battery maximum power/capacity ratio

$\overline{SG_t}$ Normalized solar gen. at t (kWh/kW installed)

$MiSoc$ Minimum battery state-of-charge ($[0, 1]$)

M A sufficiently large number

$\zeta_{n,c}$ Number of consumers of type c in node n

Φ_c Optimal investment solution for consumer type c

Ψ_c Optimal investment costs for consumer type c

Ω_c Optimal annual savings for consumer type c

γ_{pur} purchase factor used in solar compensation analysis

γ_{pk} peak factor used in time differentiation of energy costs analysis

Decision Variables

$x_{n,c}$ Peak power of consumer type c in node n

ue_t Electricity export to utility at time t (kW)

α Charging/discharging aux. variable (binary)

$\beta_{n,c}$ Binary variable indicating the presence of consumer c in node n

cap_k Installed capacity of technology k (kW/kWh)

pur_k Investment decision for tech. k (binary)

pv_t PV output at time t (kW)

ch_t Battery charge at time t (kW)

dch_t Battery discharge at time t (kW)

soc_t Battery state of charge at time t (kWh)

ui_t Import from utility at time t (kW)

Random Variables

$\text{viol}_{lim}^{\text{avg}}(\mathbf{I})$ Average magnitude of violations of system operating limit *lim* over all time points (kW).

$\text{viol}_{lim}^{\text{max}}(\mathbf{I})$ Largest magnitude of violations of system operating limit *lim* over all time points (kW).

$\text{viol}_{lim}^{\text{N}}(\mathbf{I})$ Number of violations of system operating limit *lim* over all time points, as a function of stochastic investment decisions (kW).

$I_u, \mathbf{I}$ Investment decision by customer k, also as a vector of decisions for all u.

$u_{t,u}(I_u)$ Netload seen from the utility at time t from consumer u, as a function of a stochastic investment decision (kW).

$W[A]$ Indicator random variable which has value 1 if event A occurs and 0 otherwise.

1. Introduction

Electricity tariffs are a main economic driver for the adoption of Distributed Energy Resources (DERs), namely photovoltaic (PV) and storage systems, by private consumers and microgrid owners. In fact, utility rate design decisions around different tariff components - volumetric rates, demand charges, feed-in compensations, etc. - affect the economic viability of DER technologies, encouraging or discouraging behind-the-meter investments [1, 2]. The last decades of DER policies have shown a significant increase of PV adoption in residential buildings encouraged by a portfolio of tariffs comprising net-metering schemes [3, 4, 5] and PV feed-in remuneration [6, 7]. In contrast, tariff mechanisms that impose restrictions to the PV injection, such as net-billing schemes promoting self-consumption [8, 9], lead to a limited increase of PV adoption [10].

As storage costs continue to fall, an analogous behaviour can be expected in the behind-the-meter adoption of these technologies. In fact, private storage adoption, when combined with PV, has the potential to increase consumers' self-sufficiency [11, 12] and decrease their energy bill. Additionally, new revenue streams for storage appear when tariffs comprise a significant time differentiation of energy costs, e.g. time-of-use (ToU) rates or real-time prices [13], or when batteries are used to decrease peak demand charges [14, 15]. Thus, these time-dependent characteristics of the electricity tariffs can be another driver for the adoption of behind-the-meter storage installations and influence the dispatch of these assets. These temporal characteristics of tariffs are considered in many storage scheduling [16] and sizing [17] methods as well as in prosumer and microgrid DER adoption models [18, 19].

The potential of rate design to drive long-term behind-the-meter adoption of PV and storage technologies has been explored by several authors in the literature, for example to understand the effectiveness of financial subsidies in promoting DER technologies [20], to discuss grid cost recovery in scenarios of massive penetration of PV and storage [21, 22, 23] and to quantify the relationship between rate design and ancillary services costs at the distribution grid level [24]. However, most of the contributions in this domain are made from a pure economic perspective, neglecting some of the well known physical impacts of the presence of DERs (PV in particular) on the distribution network operation, such as overvoltages or voltage unbalances [25, 26].

On the other hand, the security aspects of the distribution grid associated with the massive adoption of PV have been treated in a more technical perspective, for example through different probabilistic load flow (PLF) methods, applied to utility grid planning [27, 28] and operations [29, 30] in order to quantify the impact of prosumers' DER adoption and new PV connections into the distribution grid. Some of these PLF methods, e.g. [31], capture the intermittence and short-term uncertainty of the PV production and the consequent impact on voltages and line flows of the distribution network. However, in a longer time scale, these models neglect the economic dynamics of the PV and storage adoption and the role of electricity tariffs in driving the behind-the-meter installations of these DERs with significant impacts to the grid operation.

In short, the literature on DER policy and economics claims that electricity tariffs are a main driver of the behind-the-meter adoption of PV and storage, with the ability to influence dispatch of these technologies and dramatically change the netload in different nodes of the distribution network. At the same time, a comprehensive literature on power distribution studies has pointed out that an uncontrolled adoption of these resources (especially PV) can introduce new security and power quality challenges in the steady-state conditions of the distribution grid, which requires new system planning methods [32]. From these two perspectives, it is clear that rate design decisions now have the potential to impact the grid in the future, if the economic dynamics of DER adoption are taken into account. However, as these two lines of research have evolved separately, only a reduced number of studies have focused on this impact [21, 22, 23, 33, 34].In particular, a methodology to quantify the grid security and reliability impacts of tariff driven adoption of solar technologies was presented in [33, 34] and [35], respectively. In these papers, the authors used an optimization-based approach, from the prosumer perspective, to calculate the post-adoption netload and the consequent impact on the grid. Although [33, 34] have the merit of being the first attempt to measure this phenomenon, this approach fails to capture the uncertainty of DER adoption decisions, which may result in an unrealistic evaluation of the grid impacts, especially in systems with a large number of potential prosumers. Thus, to address this problem in a realistic manner, this paper contributes to the literature on the field by presenting a methodology to quantify the impact of the electricity tariffs on the long-term steady state security conditions of the distribution grid. To achieve this, this paper proposes a new hybrid stochastic adoption model that fit the specific objectives of this work and facilities integration with a PLF evaluation. The contributions of this paper are threefold:

- First, to propose an extension to the analysis of [33, 34] by capturing the uncertainty of DER adoption when calculating the effect of electricity tariffs on the netload profiles of the potential prosumers;
- Second, to translate this uncertainty at the different nodes into a probabilistic impact analysis of the grid security conditions, using a PLF algorithm to calculate voltage and line flow distributions. The end result is a full probabilistic model that captures the long-term economic impact of rate design on the steady state adequacy of the distribution grid.
- Finally, to perform a sensitivity analysis to the different components of the rate design and evaluate their probabilistic impact on the grid voltages. To do that, a case study involving a set of prototypical consumers in California and a MV distribution network with 118 nodes is presented.

The rest of the paper is organized as follows: Section 2 presents an overview of the methodology of this paper and discusses its underlying assumptions; Section 3 proposes a stochastic adoption model for PV and storage technologies with the purpose of evaluating the impact of tariffs offered by the utility; Section 4 describes the PLF analysis based on the Monte Carlo method; Section 5 provides a case study and presents the results to illustrate the methodology proposed; finally, Section 6 presents the main conclusions of the paper.

2. Methodology Overview

Capturing the effect of electricity tariffs and DER technology costs on the long-term security of the distribution network requires an integration of DER adoption models (representing the prosumers' side) with load flow calculations that are able to estimate the steady-state conditions of the distribution grid on the

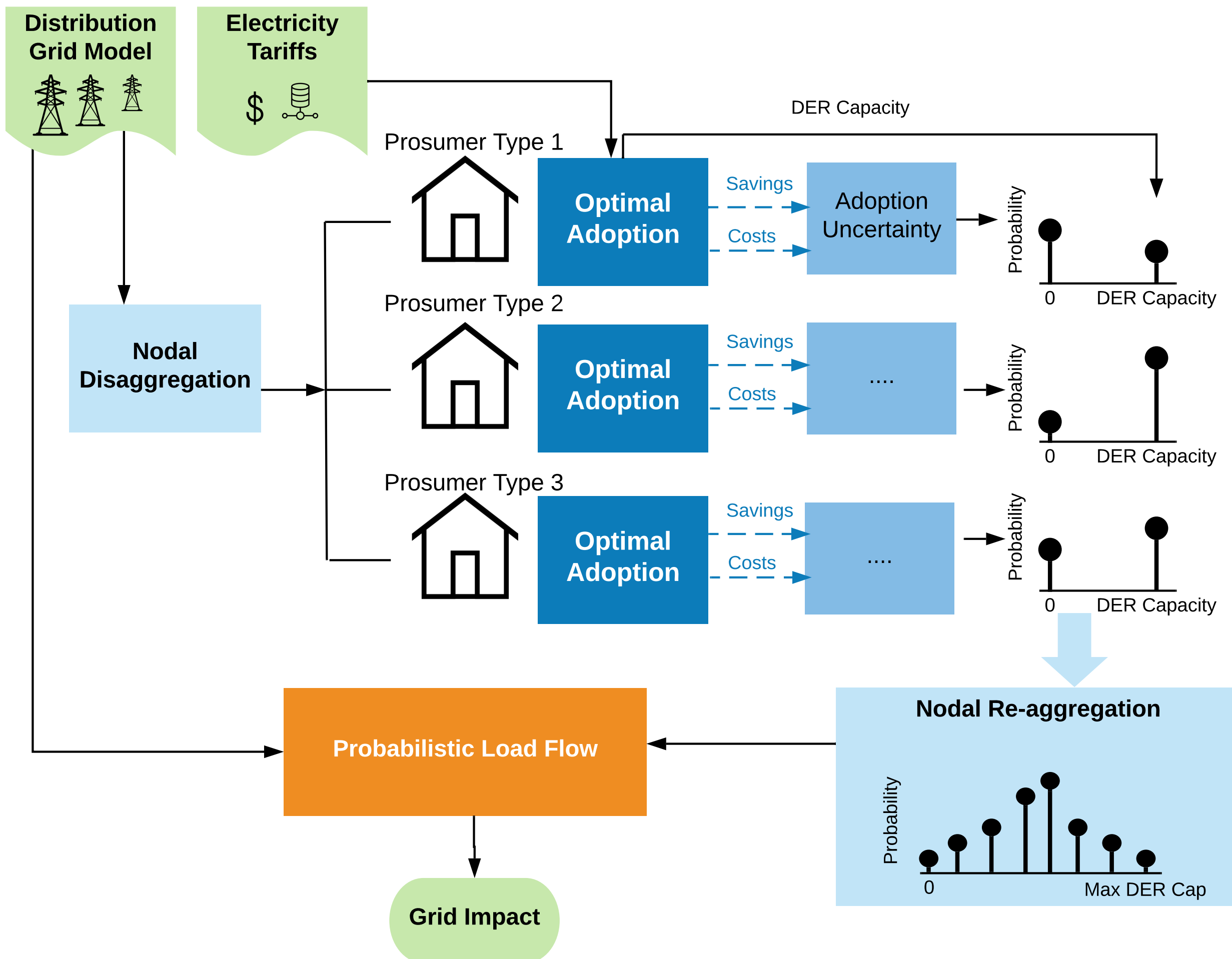

Figure 1: Overview of the Methodology

long run. The methodology proposed in this paper extends the work presented in [33, 34] by considering the uncertainty of DER adoption decisions made by individual consumers and integrating it with an stochastic evaluation of the grid security. Therefore, two types of inputs are taken to perform this analysis: 1) the distribution network circuit model to be evaluated by the grid planners; 2) a set of electricity tariffs, including different tariff components (e.g. time-of-use rates, peak demand costs, PV compensation rates) as well as other economic parameters such as technology costs. The main output of this analysis is the long-term probability distribution of voltage and line flows and the consequent risk of violation of standard security limits.

Fig. 1 presents an overview of the methodology. As shown in the figure, the first step consists of disaggregating the different nodes of the distribution grid into representative consumer types that are typically categorized by the utility in the rate design process. Second, the economic scenarios of technology costs and electricity tariffs are used to build an adoption model for each type of consumer in order to identify the optimal level of PV and storage investments for each group. Then, these representative results are taken as a reference to model the stochastic decisions of each individual consumer and, later, to characterize the uncertainty of the DER capacities at each node of the distribution network. Finally, a PLF algorithm is run to obtain long-term voltage and line flow probability distributions from these netload nodal uncertainties.

It is important to note that the PLF evaluation employed in this work implies a different time-scale and a different uncertainty characterization when compared with other probabilistic analysis in the context of DER deployment in distribution grids. In fact, most of the PLF algorithms in this domain [29, 27, 30, 28, 31] are focused on shorter term aspects of decentralized PV and load uncertainty (related with intra-day consumption variations, radiation intermittence, etc.), which are relevant for operations and operational planning problems and widely used to support decisions made hours/minutes ahead of the uncertainty realization. In contrast, the proposed methodology is designed to capture long-term uncertainties associated with tariff driven adoption of DERs in a planning horizon, i.e. projecting netload scenarios to support economic and infrastructural strategic decisions made several years ahead of the uncertainty realization. Hence, for the purposes of this paper, the intra-day uncertainty of the PV generation is ignored, and only its hourly expected values of PV production are considered to build the design days for grid planning. The objective of this simplification is to keep the focus on the uncertainty that matters in the context of infrastructural planning, economic assessment and rate design. Nonetheless, it is important to emphasize that the methodology proposed is agnostic to this simplification, as the Monte Carlo based PLF presented below can be expanded to accommodate a full scenario tree with intra-day realizations of solar generation.

3. Prosumer Adoption Model

In the literature, two types of approaches exist to estimate future adoption of DER technologies. The first is assuming economic rationality in long-term consumers' decisions related to the acquisition and utilization of DER assets. These models are very popular for designing and predicting investments in DER infrastructure in buildings and microgrids, e.g. [18, 19], and are widely used to estimate future adoption and netload when the number of consumers in a particular node is relatively low [33, 34, 35]. This economic rationality is typically represented as an optimization model, simulating optimal decisions from the perspective of the prosumers, including the size and dispatch of the DER assets in ways that minimize prosumers' overall energy bill. Thus, by running these behind-the-meter optimizations for a set of potential electricity tariffs offered by the utility, it is possible to understand how the rate design process triggers economic responses from the prosumers' side, which translates into new DER investments and consequently into netload changes in the nodes of the distribution grid. However, the assumption behind these models, i.e. the economic rationality, is not always representative of the consumers decisions. In other words, evidence has shown that consumers do not adopt DERs just because it is rational to do so [36], and therefore assuming a deterministic projection based on ideal adoption may lead to significant errors in the prediction of these assets.

The alternative approach is to consider socioeconomic models that describe adoption and diffusion of

DER technologies by correlating short-term social and geographical aspects of consumers' decisions. These models are typically data-driven and rely on historical information about prosumers' decisions, capturing the interplay between multiple socioeconomic factors and generating spatio-explicit patterns of future adoption [37] [38]. For example, in the case of PV diffusion, inputs of these models can include the feed-in tariffs offered by the utility [36], allowing the establishment of an empirical relationship between the rate design process and the DER adoption. Nonetheless, these models require a significant amount of information that is not always available to utilities, such as geographical characterization of specific regions or the socioeconomic factors that motivated the adoption decisions. Additionally, these data-driven methods may be inaccurate to predict DER penetration in situations where conditions of adoption change dramatically and past data is no longer valid to project the future. This is the case of the application studied in this paper, where adoption models are used to test the impact of innovative electricity rate design strategies, that may comprise radical changes in the tariff components and, consequently, in the consumers' economics.

In summary, socioeconomic data models have the advantage of capturing the uncertainty associated with the subjectivity of the prosumers' decisions, but they are limited solutions when the economic conditions of adoption change dramatically. In contrast, approaches based on economic rationality can be more adequate for those cases, but they fail to model uncertainty in a realistic manner. Therefore, this section presents a hybrid model for PV and storage adoption developed for the purpose of the long-term rate design and grid planning analysis presented in this paper. This adoption model combines proprieties of both economic rationality and socioeconomic diffusion models with the objective of representing consumers' rational responses to electricity tariffs in the long run while considering the uncertainty in investment decisions. As shown in Fig. 1, this model consists of three stages:

1. The load at the nodes of the distribution grid is disaggregated into prototypical consumers;
2. An economic optimization is run for each consumer with the objective of determining the rational adoption as well as the corresponding investment costs and savings;
3. The potential investment costs and the savings of the ideal solution are used to build a probabilistic model for the adoption.

The following subsections describe in detail each of these steps.

3.1. Disaggregation

The classification of consumers into different types is a common practice in rate design, allowing utilities to construct baseline load profiles for different classes of residential, commercial, industrial and public buildings consumers (for example, a database of load profiles for different prototypical consumers in the US is available in [39]). However, the way these consumers are distributed throughout the nodes of the distribution feeders might be unknown or at least difficult to estimate for some utilities. In that case, based on the observation of the real load profile, a simple disaggregation method can be applied.

For a distribution grid with a set of nodes $\mathcal{N}$, considering a set of prototypical consumers $\mathbb{C}$, each with a normalized load profile described by $\overline{LC_{c,t}}$, the power of each consumer type in each node $x_{n,c}$ is given by the optimization model presented in (1)-(5). The objective function minimizes the disaggregation error in relation to the preexisting network load $L_{n,t}$. Constraints (2) and (3) impose a ratio in each node between the peak load of residential and services buildings. In practical applications, this ratio can be obtained based on the installed power information of residential and commercial consumers connected to each node. Constraints (4) and (5) guarantee a minimum reference average power for each consumer type PR_c, in case the consumer exists in node n.

$$min \sum_{n \in \mathcal{N}} \sum_{t \in \mathcal{T}_{yr}} \Big(\sum_{c \in \mathbb{C}} \overline{LC_{c,t}} \cdot x_{n,c} - L_{n,t} \Big)^2 \tag{1}$$

$$\sum_{c \in \mathbb{C}_R} x_{n,c} \leqslant \sum_{c \in \mathbb{C}_S} x_{n,c} \cdot SR_n \cdot (1 + E_{sr}) \tag{2}$$

$$\sum_{c \in \mathbb{C}_R} x_{n,c} \geqslant \sum_{c \in \mathbb{C}_S} x_{n,c} \cdot SR_n \cdot (1 - E_{sr}) \tag{3}$$

$$x_{n,c} \geqslant PR_c \cdot \beta_{n,c} \cdot (1 + E_{pr}) \tag{4}$$

$$x_{n,c} \leqslant \beta_{n,c} \cdot \mathrm{M} \tag{5}$$

With this disaggregation, the total number of consumers of type c in node n, $\zeta_{n,c}$, can be approximated by:

$$\zeta_{n,c} = \frac{x_{n,c}}{PR_c} \tag{6}$$

3.2. Economic Rational Adoption

Prototypical consumers have different load shapes and magnitude of demand, which creates different conditions for adoption of PV and storage technologies. Hence, it is expected that some types of consumers tend to adopt more of these technologies than others, just due to the characteristics of their load profiles and the nature of the consumption (for example, in some cases commercial and industrial consumers are eligible to more favourable solar compensation rates than residential consumers). As discussed above, this is the rational component of adoption that is captured in this step of the model, by creating a reference solution for adoption of PV and storage technologies for each consumer type. This reference allows an understanding of how different classes of consumers may respond with investments to specific variations in the tariffs offered by the utility. Later, this reference of economic rational adoption will be used to build a probabilistic model describing the decisions of individual consumers within each class.

To capture the economic rationality of the adoption we use the optimization framework derived from the Distributed Energy Resources Customer Adoption Model (DER-CAM) proposed in [18, 19] and used in the context of multi consumer adoption in [33, 34]. Thus, for each consumer type c, the ideal capacity of technology k to adopt, cap_k, can be obtained by solving the optimization model (7)-(15). The objective function (7) minimizes the fixed variable costs for investments in DERs, considering an equivalent annual cost (EAC) model, where asset investments are annualized based on the coefficient Ann_k. The cost function also takes into account the annual costs of energy and the remuneration paid by the utility for the energy injected into the grid.

$$
\begin{aligned}
min \sum_{k\in\{s,pv\}} & \Big(CFix_k \cdot pur_k + CVar_k \cdot cap_k\Big) Ann_k \\
+ & \sum_{t\in\mathcal{T}_{yr}} (ui_t \cdot EC_t - ue_t \cdot FI_t)
\end{aligned}
\tag{7}
$$

Constraints of the problem include the fixed cost condition of the investments (8). Hourly operation of the battery is constrained by the well known reservoir model (9), the storage capacity (10) limits and the power limits (11) associated with the maximum battery discharge rate PCr, as well as inequalities precluding simultaneous charging and discharging (12)-(13). PV generation is limited by the installed capacity and the solar radiation (14). Equation (15) imposes the energy balance of the system.

$$cap_k \leqslant pur_k \cdot \mathrm{M} \tag{8}$$

$$soc_t = soc_{t-1} + ch_t \cdot CEff - \frac{dch_t}{DEff} \tag{9}$$

$$MiSoc \cdot cap_s \leqslant soc_t \leqslant cap_s \tag{10}$$

$$ch_t, dch_t \leqslant cap_s \cdot PCr \tag{11}$$

$$ch_t \leqslant \alpha \cdot \mathrm{M} \tag{12}$$

$$dch_t \leqslant (1-\alpha) \cdot \mathrm{M} \tag{13}$$

$$pv_t \leqslant cap_{pv} \cdot \overline{SG_t} \tag{14}$$

$$LC_t = ui_t - ue_t + pv_t + dch_t - ch_t. \tag{15}$$

After solving the model (7)-(15) for each consumer type c connected to the utility network, it is possible to obtain the ideal investment solutions Φ_c as well as the optimal investment costs Ψ_c and the annual savings Ω_c that serve as a reference for each consumer class:

$$\Phi_c = \{cap_{c,k}, pur_{c,k}\} \;\; \forall k \in \mathbb{K} \tag{16}$$

$$\Psi_c = \sum_{k\in\{s,pv\}} CFix_k \cdot pur_{c,k} + CVar_k \cdot cap_{k,c} \tag{17}$$

$$\Omega_c = \sum_{t\in\mathcal{T}_{yr}} EC_t \cdot LC_t - ui_t \cdot EC_t + ue_t \cdot FI_t \tag{18}$$

3.3. Probabilistic Adoption of Individual Consumers

Having established the reference of economic rational adoption, the next step of the model aims at representing each consumer's uncertain decision with a probabilistic model. After calculating the reference for each consumer class, the DER investments of a particular consumer, u, are described as a random variable following a Bernoulli distribution with probability determined by the costs and savings associated with the DER, shown in (19). We define I_u as the adoption random variable for consumer u, so that adoption is realized as $i_u = 1$ when the DER is adopted and $i_u = 0$ when it is not. The probability of a specific consumer u in class c to adopt the DER reference solution of the class, Φ_c, is given by p_c.

$$I_u \sim \text{Bernoulli}(p_c), \quad \forall u \in c \tag{19}$$

To estimate the probability of adoption of an individual consumer, we take into account the reference costs and savings of the prototypical class, c, where the consumer is included. This cost-savings model describes the potential benefit to be realized from adoption, φ_c, as a function of the capital cost Ψ_c, annual avoided cost of energy, Ω_c, and a customer-specific fixed effect FE_c, according to (20).

$$\varphi_c = \beta_1 \ln \Psi_c + \beta_2 \ln \Psi_c^2 + \beta_3 \ln \Omega_c + FE_c \tag{20}$$

As seen in the model, the terms β_1, β_2, β_3 can be obtained based on the statistical observations of past adoption of PV and storage technologies in each consumer class. In the context of energy conservation adoption, Anderson and Newell [40] parameterized a similar model (also based on a Bernoulli distribution) using a dataset with more than 70,000 energy conservation measures recommended by energy audits in small and medium-sized industrial firms in the United States from 1981 to 2000 and whether or not each was adopted. Obviously, in the domain of PV and storage investments by private consumers the parameterization will be different, as it depends on other socio-economic factors. However the process is similar and in both cases the stochastic model is built around a reference of economic rationality and parameterized with statistical observations. The fundamental difference is that, in the proposed model, the rationality of adoption of Anderson and Newell [40] (the recommended audits) is replaced by the optimal PV and storage adoption of each prosumer class (here determined via an optimization model).

After defining the benefit of adoption of each class, φ_c, a logit model is used to obtain the probability of adoption as shown in (21).

$$p_c = \frac{\exp(\varphi_c)}{1 + \exp(\varphi_c)} \tag{21}$$

It is important to note that the fixed effect FE_c can be used to shift the model for a specific firm or situation to match a known adoption probability, μ, at a particular savings B_0 and cost C_0, as shown in (22).

$$FE_c = \ln\left(\frac{\mu}{1-\mu}\right) - \beta_1 \ln C_0 - \beta_2 \ln C_0^2 - \beta_3 \ln B_0. \tag{22}$$

4. Probabilistic Load Flow

When the long-term netload profiles of consumers are probabilistic, subject to the uncertain adoption of PV and storage technologies, appropriate system planning requires means to translate these probabilistic profiles at the consumer nodes into probability distributions of variables in the system. In particular, it is important to obtain distributions of certain system performance metrics, such as the frequency and severity of violations of system operating limits. These distributions are given by PLF methods based on advanced sampling [41] and non-sampling [42] approaches. To simplify the explanation of the PLF methods within the scope of this work, this chapter presents a simple Monte Carlo simulation that solves the AC power flow equations in each trial, considering as an input the probabilistic adoption model presented in the previous chapter.

4.1. Monte Carlo Simulation

A Monte Carlo simulation is developed to obtain probabilistic information about the effects of the adoption of DERs under this probabilistic model. Each customer with an investment option presents one random variable, i_u. As discussed above, neglecting uncertainty in load and operations of PV and storage, the customer's netload seen from the utility grid takes one of two profiles, depending on the investment decision, as in (23).

$$u_{t,u}(I_u) = \begin{cases} u_{t,u}^{\text{base}}, & I_u = 0 \\ u_{t,u}^{\text{adopt}}, & I_u = 1 \end{cases} \tag{23}$$

where the term $u_{t,u}$ represents the total netload of the consumption derived from the model (7)-(15) applied to the class c, in which the consumer is included, as defined in (24).

$$u_t = ui_t - ue_t \tag{24}$$

At any point in time, the probability that the customer's import takes a certain value depends only on the probability of adoption, shown in (25).

$$P\left(u_{t,u}(I_u) = u_{t,u}^{\text{adopt}}\right) = p_c, \quad \forall t \in \mathcal{T}_{yr}, \quad \forall u \in c \tag{25}$$

The dependence between the input random variables across time points must be taken into account when finding the output probability densities, in order to allow for risk metrics that incorporate multi-temporal behavior, including the storage dispatch. Maintaining this dependence, each input and output profile is a random vector of $|\mathcal{T}_{yr}|$ elements.

We denote the vector of the adoption variables for each customer as $\mathbf{I}$. In each Monte Carlo trial, j, and construct a realization $\mathbf{i}_j$ of this vector by sampling from a standard uniform distribution independently for each consumer and comparing to the customer's adoption probability, p_k. Using the load profiles corresponding to this realization, an AC power flow is solved for each time t in the set of all time points $\mathcal{T}_{yr}$ to obtain profiles of the system variables for the full period.

These trials are repeated with a different realization each of n times until the variance of the estimators of interest decreases sufficiently. Each trial result is used to construct estimators for distributions described in the following section.

4.2. Monte Carlo Estimators

The Monte Carlo simulation gives estimators for the output random variables of interest. Here we consider several which can be useful in multi-temporal risk metrics. Each of the following variables apply to a single operating limit of one system quantity, such as the lower limit on voltage magnitude at a single bus or upper limit on the power flow on a single branch.

In the following, we denote the variable Z and the limit value z_{lim}, and we use notation of upper limits for all variables, so that $Z - z_{lim} > 0$ always means a threshold violation. If z_{lim} is a lower limit, both Z and z_{lim} are multiplied by -1 before the following equations are applied.

Finally, the generic random variable, W, indicates the limit violations. Thus, the variable $W[Z_t > z_{lim}]$ has value 1 if Z_t violates z_{lim} and 0 otherwise.

4.2.1. Number of Violations

The number of violations over all time periods of variable Z with limit z_{lim}, given the state of adoption of all customers, $\mathbf{I}$, is denoted by $\text{viol}^{\text{N}}_{lim}(\mathbf{I})$. Equation (26) gives this value.

$$\text{viol}^{\text{N}}_{lim}(\mathbf{I}) = \sum_{t \in \mathcal{T}_{yr}} W[Z_t(\mathbf{I}) > z_{lim}] \tag{26}$$

The estimates of the probability density function (pdf) and cumulative distribution function (cdf) are constructed by the Monte Carlo estimator for the number of violations. The indicator variable $W[\text{viol}^{\text{N}}_{lim} = m]$ indicates whether the number of violations has a certain nonnegative integer value m. The pdf of the number of violations is given by equation (27) and the estimated pdf after n Monte Carlo trials by $\hat{f}$ in (28).

$$f_{N_{\text{viol}}}(m) = P(\text{viol}^{\text{N}}_{lim} = v) = \mathbb{E}\left[W\left[\text{viol}^{\text{N}}_{lim}(\mathbf{i}_j) = m\right]\right] \tag{27}$$

$$\hat{f}_{\text{viol}^{\text{N}}_{lim}}(m) = \frac{1}{n}\sum_{j=1}^{n} W\left[\text{viol}^{\text{N}}_{lim}(\mathbf{i}_j) = m\right] \tag{28}$$

4.2.2. Average Violation

The average violation is denoted by $\text{viol}^{\text{avg}}_{lim}(\mathbf{I})$. This is a random variable representing the average of all the violations over the entire period, only considering the time points at which violations occur. Equation (29) gives this value.

$$\text{viol}^{\text{avg}}_{lim}(\mathbf{I}) = \frac{1}{\text{viol}^{\text{N}}_{lim}(\mathbf{I})} \sum_{t \in \mathcal{T}_{yr}} \max(Z_t(\mathbf{I}) - z_{lim}, 0) \tag{29}$$

The estimates of the probability density function (pdf) and cumulative distribution function (cdf) are similarly constructed by the Monte Carlo estimator for the average violations, with the difference that the random variable is not restricted to integers but can take any nonnegative real values. The indicator variable $W\left[\mathrm{viol}_{lim}^{\mathrm{avg}} = v\right]$ indicates whether the average violation has a certain magnitude v, shown in (30), the pdf of the average violation. The estimate for this after n Monte Carlo trials is given by (31).

$$f_{\mathrm{viol}_{lim}^{\mathrm{avg}}}(v) = P(\mathrm{viol}_{lim}^{\mathrm{avg}} = v) = \mathbb{E}\left[W\left[\mathrm{viol}_{lim}^{\mathrm{avg}}(\mathbf{i}_j) = v\right]\right] \tag{30}$$

$$\hat{f}_{\mathrm{viol}_{lim}^{\mathrm{avg}}}(v) = \frac{1}{n}\sum_{j=1}^{n} W\left[\mathrm{viol}_{lim}^{\mathrm{avg}}(\mathbf{i}_j) = v\right] \tag{31}$$

4.2.3. Maximum Violation

Similarly, we denote the largest violation over all time periods by $\mathrm{viol}_{lim}^{\mathrm{max}}(\mathbf{I})$, given by (32).

$$\mathrm{viol}_{lim}^{\mathrm{max}}(\mathbf{I}) = \max_{t\in\mathcal{T}_{yr}}\left(\max\left(Z_t(\mathbf{I}) - z_{lim}, 0\right)\right) \tag{32}$$

The pdf is given by (33) and estimated from the n Monte Carlo trials as shown in (34).

$$f_{\mathrm{viol}_{lim}^{\mathrm{max}}}(v) = P(\mathrm{viol}_{lim}^{\mathrm{max}} = v) = \mathbb{E}\left[W\left[viol_{lim}^{\mathrm{max}}(\mathbf{i}_j) = v\right]\right] \tag{33}$$

$$\hat{f}_{\mathrm{viol}_{lim}^{\mathrm{max}}}(v) = \frac{1}{n}\sum_{j=1}^{n} W\left[\mathrm{viol}_{lim}^{\mathrm{max}}(\mathbf{i}_j) = v\right] \tag{34}$$

5. Case Study

5.1. Case Study Description

This section presents a case study to evaluate the probabilistic impact of different components of the electricity tariffs on the voltage profiles of the distribution grid, considering stochastic long-term adoption of PV and storage technologies by private consumers.

The network described in Fig. 2, taken from [43], is used for the analysis presented in this section. The original load at each node of the distribution network was considered to disaggregate the nodal consumption into different prototypical consumer profiles using the method presented in section 3.1. 5 different classes of buildings were obtained in this disaggregation process, using the load profiles from the US Department of Energy Reference buildings database, assuming the climate zone of San Francisco [39]. These buildings were divided into two residential (”ResidHigh”, ”ResidLow”) and services (”hospital”, ”Secondary School”, ”Small Office”) categories. The disaggregation results for each node can be seen in Fig. 3. Finally, the annual PV radiation data was obtained from Typical Meteorological Year dataset for the same San Francisco area [44].

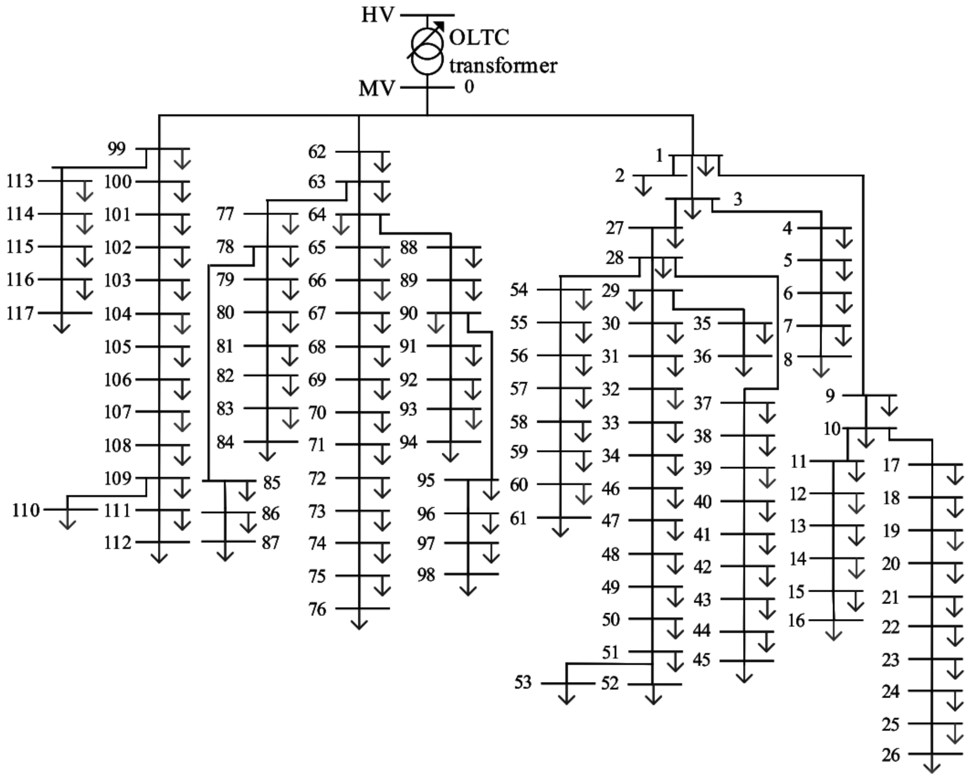

Figure 2: Medium voltage distribution network with 118 buses

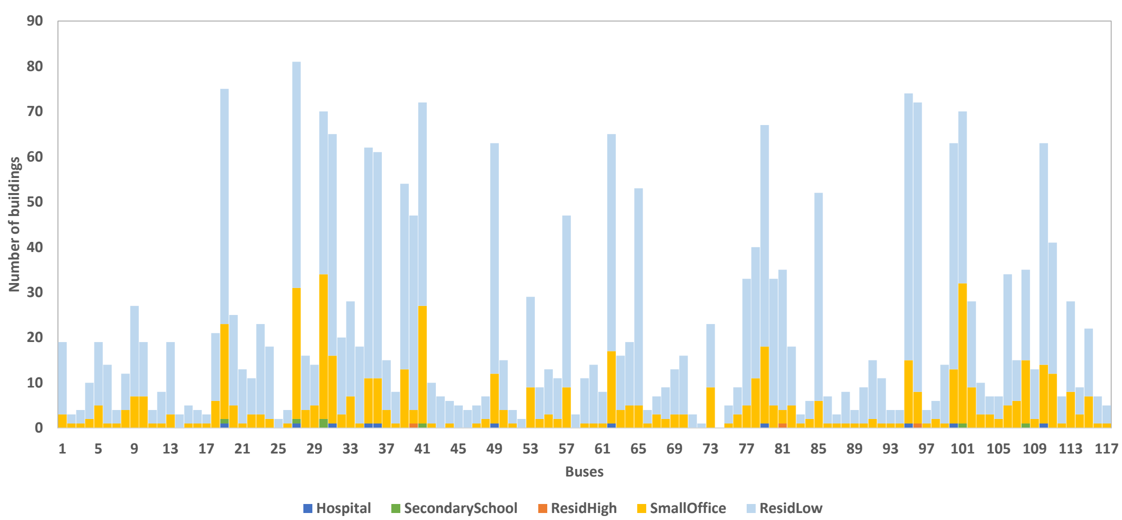

Figure 3: Disaggregation of buildings per bus

The time-of-use (ToU) rates applied to residential (”ResidHigh”, ”ResidLow”) and services (”hospital”, ”Secondary School”, ”Small Office”) building are presented in table 1. These rates are divided into Summer and Winter periods. Summer rates (from May to October) have a three segment tariff structure, divided into peak, mid-peak and off-peak rates, while Winter rates (from November to April) only have two tariff

Table 1: Base tariff rates and periods for different classes of consumers

Type	Weekdays	Weekends	Summer ($/kWh)	Winter ($/kWh)
	Residential Tariff		May-Oct	Nov-April
Peak	1:00pm - 6:00pm	—	0.39096	—
Mid-peak	10:00am - 1:00pm 7:00pm - 9:00pm	—	0.27253	0.21847
Off-peak	All other times	All times	0.197307	0.20164
	Small Commercial Tariff		May-Oct	Nov-April
Peak	noon - 6:00pm	—	0.28560	—
Mid-peak	8:00am - noon 6:00pm - 9:00pm	—	0.26195	00.24134
Off-peak	All other times	All times	0.23459	0.22043
	Medium Commercial Tariff		May-Oct	Nov-April
Peak	noon - 6:00 pm	—	0.23427	—
Mid-peak	8:00am - noon 6:00pm - 9:00pm	—	0.17914	0.14974
Off-peak	All other times	All times	0.15107	0.13268

segments, the mid-peak and off-peak. The peak time for commercial services is from 12 a.m. to 6 p.m. and for residential services is from 1 p.m. to 7 p.m.

Regarding costs of behind-the-meter technologies, a fixed installation cost of 2000 $ and a variable cost of 2500 $/kWh were assumed for PV systems with a lifetime of 20 years. Storage variable cost was assumed to be 250 $/kWh, considering a lifetime of 10 years, a charging/discharging efficiency of 90%, a maximum discharge rate of 0.3kW per kWh installed, and a minimum state of charge of 20%. The parameterization of the stochastic model, representing the adoption probability as a function of the solution costs, is presented in equation (35), considering that the fixed effect is set to zero. The probability of adoption is then found given the capital cost, $C_{cap,k}$, and annual avoided cost of energy, $A_{ann,k}$ as shown in Fig. 4.

$$\begin{aligned} \beta_1 = &\quad -0.25 \\ \beta_2 = &\quad -0.11 \\ \beta_3 = &\quad 0.6 \end{aligned} \tag{35}$$

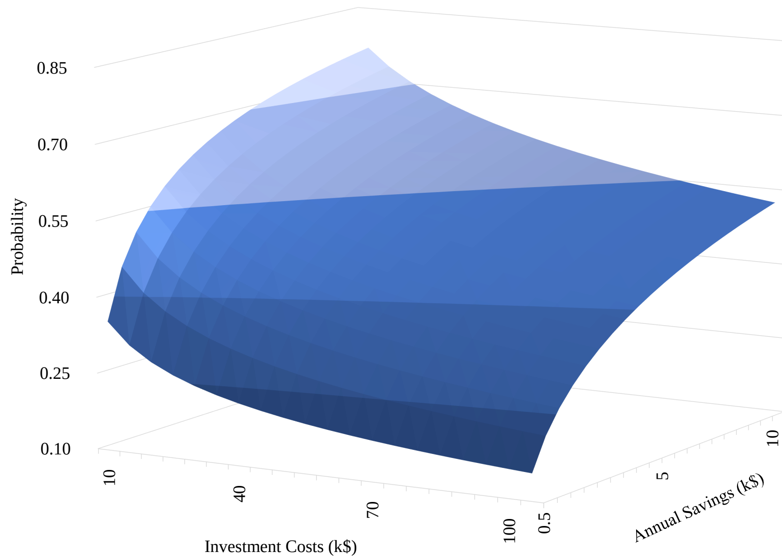

Figure 4: Probability of adoption of resources, given the annual savings and investment costs

In the remaining part of this section, the effect of different tariff components is analyzed, namely the cost differentiation of the ToU tariff and the solar compensation rate. The probability distribution results are presented in form of a box plot representing the different quartiles of the distribution.

5.2. Impact of solar compensation rates

This results subsection starts by analyzing the long-term impact of the solar compensation rate policy on the voltage profiles of the distribution grid. Mathematically, we define this compensation based on the electricity volumetric cost as follows: $FI_t = \gamma_{pur}.EC_t, \quad \forall t \in [0, T]$, where γ_{pur} is the utility solar purchase factor. In other words, when the factor is 1 the solar compensation is equal to the energy costs (net-metering scheme), and when this factor is 0.5 it means that the solar injection is remunerated at 50% of the electricity cost of the tariff. Thus, we assume a variation of γ_{pur} between 0 and 1, with steps of 0.25. Then, we evaluate the impact on the adoption distributions of PV and storage technologies by private consumers and the consequent impact on the distribution grid. For this purpose, 2 scenarios are explored: 1) when only PV investments are considered; 2) when prosumers invest in both PV and storage technologies.

Fig. 5 presents the distributions of total investments in behind-the-meter PV and storage technologies that result from the different solar compensation policies as the PV purchase factor increases. It is possible to observe that if no solar compensation exists, the PV investments are higher when storage technologies are also considered. In other words, when no remuneration is due to the consumers for the PV injected into the grid, a natural incentive for self-consumption is created, which increases the value of storage assets. In fact, when compensation for solar generation is low, behind-the-meter batteries play an important role in shifting the PV generation surplus to cover electricity demand later in the day when electricity costs are higher, leveraging both the PV and storage investments. This explains the fact that storage investments are higher when no solar compensation is due to prosumers.

In contrast, when solar compensation increases, investments in PV become more attractive and storage technologies lose their value. When the purchase factor reaches 0.5 and PV is remunerated at 50% of the energy costs, storage technologies are no longer cost-effective and only PV investments can be expected from the consumers. Also, it is important to note that the uncertainty of PV investments increases (and the uncertainty of storage decreases) with the solar compensation policies.

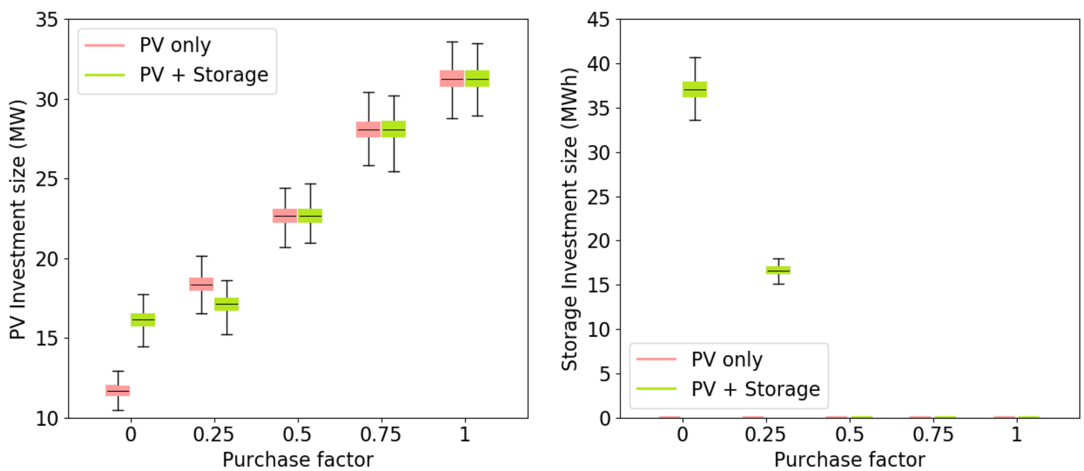

Figure 5: Distribution of PV and storage investments for different purchase factors

As expected, the different scenarios of PV and storage adoption driven by the changes in solar compensation policies have an impact on the voltage profiles of the distribution grid. When mapping this adoption across different nodes of the distribution network, it is possible to observe steady-state overvoltage violations due to the PV penetration, considering the limit of 5% of the nominal voltage. These violations start to appear when the utility purchase factor reaches 0.75, i.e. when the solar compensation represents 75% of the electricity costs. Section 4.2 presented the Monte Carlo estimators to quantify this impact considering different DER adoption realizations. In particular, we look at the average and frequency of these voltage violations (number of hours where overvoltages occur), as well as maximum violations encountered across the different nodes of the grid. Fig. 6 presents the distributions (first, second and third quartiles) of these three indices for the high values of solar compensation. It is possible to see a significant difference between the magnitude and duration of the voltage violations with just 25% variation (between 0.75 and 1) of the utility purchase factor. In fact, while these violations are relatively small for a purchase factor of 0.75, they significantly increase in number and magnitude if PV injection is remunerated at the energy price. As shown in the right-hand side plot, there is a significant probability of finding maximum violations over 1% of the nominal voltage.

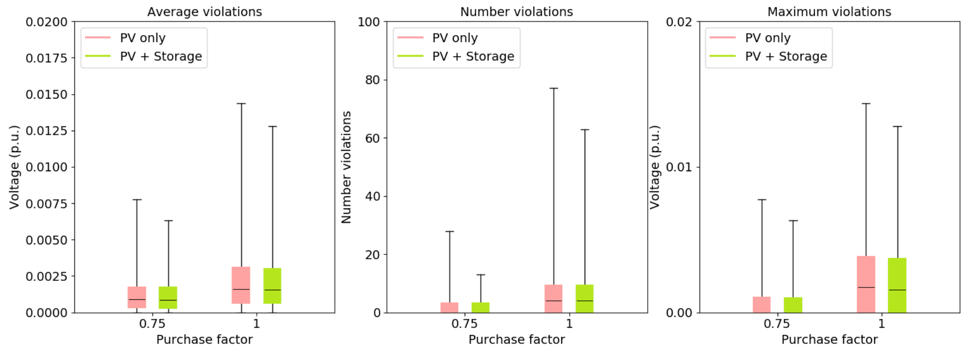

Figure 6: Distribution of number, average magnitude and maximum voltage violations for different purchase factors

Thus, by applying the methodology presented in this paper, it is possible to clearly quantify the relevant grid impacts caused by a change in the solar compensation policy adopted by the utility. In particular the probability distributions of voltage violations associated with a change in the PV purchase factor are obtained, allowing utilities to make quantitative and risk-oriented decisions around solar compensation strategies for different types of consumers.

5.3. Impact of time differentiation of energy prices

This section analyses the grid impacts caused by a modification of the time differentiation component of the electricity tariffs. ToU rates are composed by off-peak and peak rates, as seen in Table 1, which aim at providing an incentive for load shifting behaviors from the consumer side. In this analysis, the difference between these two components is modified by increasing the peak tariff in relation to the nominal values presented in table 1. Thus, we introduce a peak factor, γ_{pk}, applied to the nominal peak rate $\overline{EC_t}$ and obtain new peak scenarios as follows: $EC_t = \gamma_{pk}.\overline{EC_t}, \quad \forall t \in \mathcal{T}_{pk}$. The values of γ_{pk} vary between 1 and 2.5 with incremental steps of 0.5, while the mid-peak and off-peak tariffs remain the same. At the same time, 2 scenarios of solar compensation are defined, based on the analysis presented above (setting the utility PV purchase factor (γ_{pur}) to 0.5 and 1). It is important to stress that by increasing γ_{pk}, a double effect on the electricity costs is introduced: 1) the overall electricity costs increase at peak hours, which also implies an increase of the PV remuneration proportional to γ_{pur}; 2) the difference between peak and off-peak remuneration increases, imposing a temporal differentiation of the energy costs.

Fig. 7 presents the distribution of the behind-the-meter PV and storage capacity expected in the system for each scenario of γ_{pk} and γ_{pur}, taking into account the stochastic adoption described in Fig. 4. As shown in the figure, behind-the-meter PV installations are expected to grow as the electricity costs increase during the peak hours for both scenarios of γ_{pur}. However, this effect is more perceptible in the adoption of storage technologies that become cost-effective when γ_{pk} is equal to 1.5 and increases exponentially for peak factors higher than this value. This means that the temporal differentiation of energy prices creates a natural incentive for energy shifting, which introduces a new value stream for storage and increases the

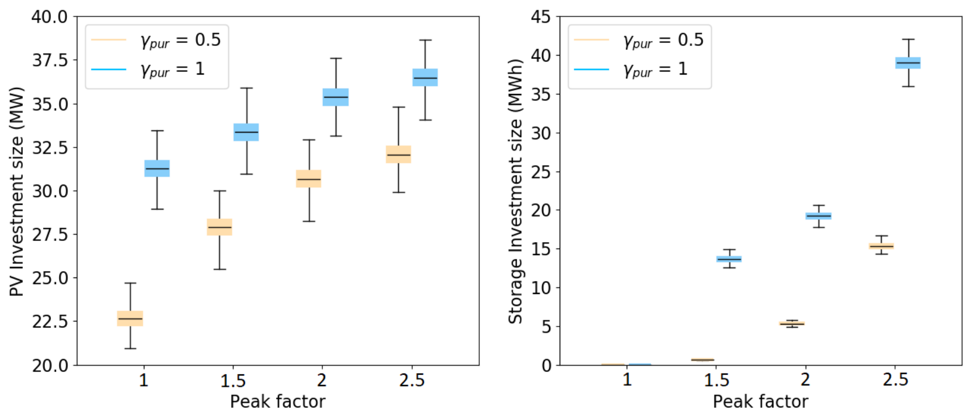

Figure 7: Capacity investments in PV and storage systems for different peak factors

probability of these technologies to be adopted by consumers.

Additionally, it is interesting to observe that the adoption of storage technologies is more evident when solar is remunerated at higher rates. This result seems counterintuitive after the analysis conducted in the previous section, where the storage value decreased with the solar compensation. This can be explained by the type of installation assumed in the model (1)-(5), which does not allow for a distinction between power injections from the battery and from the PV panel. Therefore, when a single metering point is assumed for PV and storage installation, a tariff with high solar compensation creates an additional incentive for energy arbitrage, allowing the battery to store energy during the off-peak hours and sell it during peak periods at the solar price. In fact, a simultaneous combination of high solar compensations with high temporal differentiation in the tariff leads to the perverse effect illustrated in Fig. 8, which compares the hourly netload for different scenarios of γ_{pur}. As shown in the right-hand side panel of the figure, this combination of factors not only increases the power injection during the solar hours but also creates an additional consumption in the beginning and at the end of off-peak period.

The impact of the time differentiation of energy prices on the maximum voltage violations observed in the network is depicted in Fig. 9. As expected, the voltage violations increase with the time differentiation between peak and off-peak times. Moreover, when the solar compensation is higher, violations of the minimum voltage limit are also observed due to the additional consumption that results from the energy arbitrage behaviors. Therefore, when looking at the distribution of the voltage violations (for the case γ_{pur}=1 and γ_{pk}=2.5) in Fig. 10, one can notice extreme upper limit violations during solar hours combined with lower limit violations at the beginning and at the end of the off-peak period.

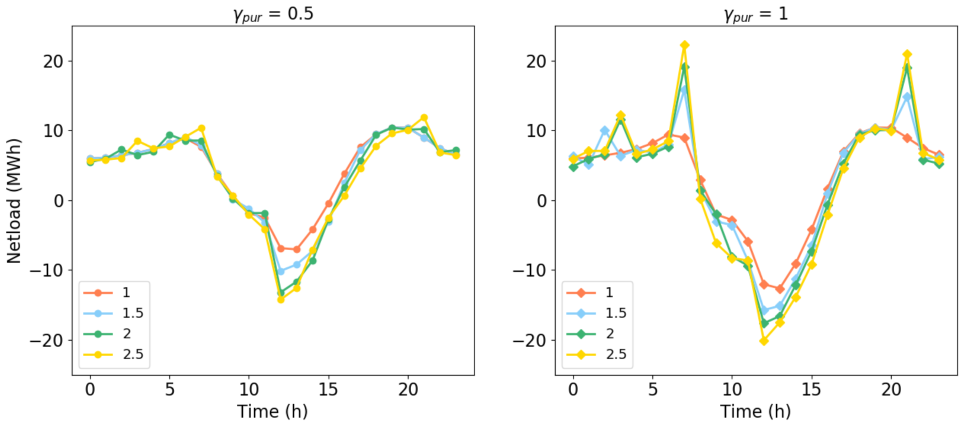

Figure 8: Average daily netload for different purchase and peak factors.

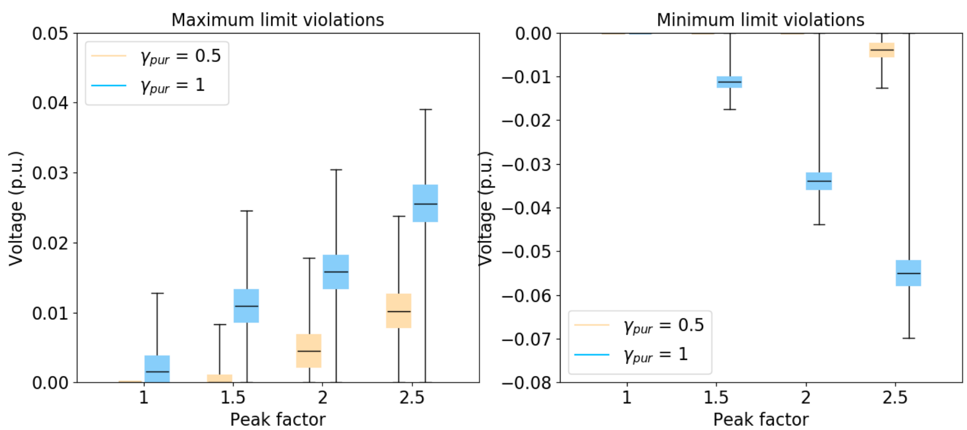

Figure 9: Distribution of maximum and minimum voltage violations for different peak and purchase factors.

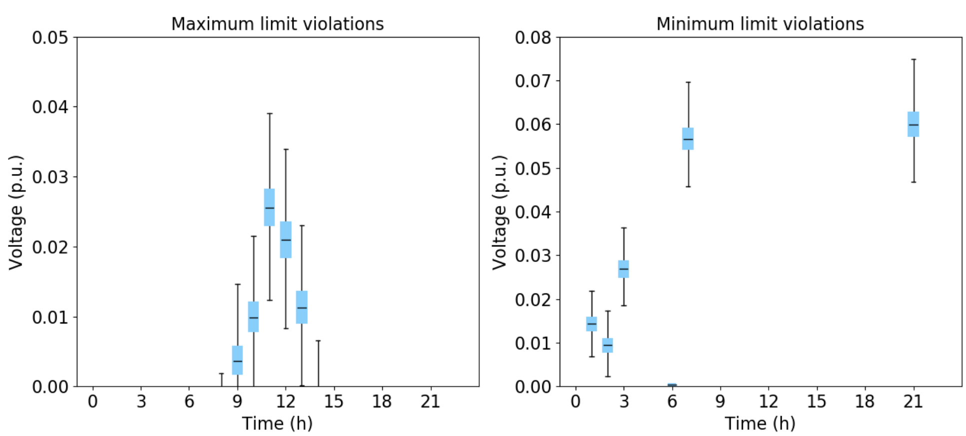

Figure 10: Distribution of the maximum and minimum voltages violation per hour with $\gamma_{pur} = 1$ and $\gamma_{pk} = 2.5$.

6. Conclusion

This paper presented a methodology to calculate the long-term effect of the rate design process on the voltages profiles of the distribution grid, considering the adoption of PV and storage technologies by private consumers. This methodology extends the existing approaches of the literature to model the stochastic nature of the individual consumers' decisions together with the economic rationality of DER investments in response to electricity tariffs. Additionally, this innovative adoption model is integrated with a probabilistic load flow evaluation to capture the grid impacts.

An analysis of behind-the-meter solar compensation mechanisms was presented, as well as the time differentiation component of ToU tariffs. It is possible to conclude that a higher solar compensation decreases the value of storage and increases the PV adoption (both the expected value and the uncertainty), leading to high probability scenarios of voltage violations. On the other hand, the time differentiation of the ToU component of the tariff increases the adoption of storage and leads to aggressive dispatch policies that can cause voltage violations of both upper and lower technical limits. In both cases, the probability distribution of voltage violations was calculated, demonstrating the relevance of the methodology in providing risk-assessment information to the utility rate design process. Thus, future works will focus on the decision-support methods that enable these applications.

Acknowledgment

The authors would like to acknowledge the Microgrids R&D and the Advanced Grid Modeling Programs of the U.S. Department of Energy - Office of Electricity, for the support granted to this work.

References

[1] R. Sioshansi, Retail electricity tariff and mechanism design to incentivize distributed renewable generation, Energy Policy 95 (2016) 498 – 508 (2016).

[2] A. Picciariello, J. Reneses, P. Frias, L. Söder, Distributed generation and distribution pricing: Why do we need new tariff design methodologies?, Electric Power Systems Research 119 (2015) 370 – 376 (2015). doi:https://doi.org/10.1016/j.epsr.2014.10.021.

[3] N. R. Darghouth, G. Barbose, R. Wiser, The impact of rate design and net metering on the bill savings from distributed pv for residential customers in california, Energy Policy 39 (9) (2011) 5243 – 5253 (2011). doi:https://doi.org/10.1016/j.enpol.2011.05.040.
URL http://www.sciencedirect.com/science/article/pii/S0301421511004265

[4] N. R. Darghouth, G. Barbose, R. H. Wiser, Customer-economics of residential photovoltaic systems (part 1): The impact of high renewable energy penetrations on electricity bill savings with net metering,

Energy Policy 67 (2014) 290 – 300 (2014). doi:https://doi.org/10.1016/j.enpol.2013.12.042.
URL http://www.sciencedirect.com/science/article/pii/S0301421513013062

[5] I. Koumparou, G. C. Christoforidis, V. Efthymiou, G. K. Papagiannis, G. E. Georghiou, Configuring residential pv net-metering policies – a focus on the mediterranean region, Renewable Energy 113 (2017) 795 – 812 (2017). doi:https://doi.org/10.1016/j.renene.2017.06.051.
URL http://www.sciencedirect.com/science/article/pii/S0960148117305566

[6] J. Ossenbrink, How feed-in remuneration design shapes residential pv prosumer paradigms, Energy Policy 108 (2017) 239 – 255 (2017). doi:https://doi.org/10.1016/j.enpol.2017.05.030.
URL http://www.sciencedirect.com/science/article/pii/S0301421517303142

[7] F. J. Ramírez, A. Honrubia-Escribano, E. Gómez-Lázaro, D. T. Pham, Combining feed-in tariffs and net-metering schemes to balance development in adoption of photovoltaic energy: Comparative economic assessment and policy implications for european countries, Energy Policy 102 (2017) 440 – 452 (2017). doi:https://doi.org/10.1016/j.enpol.2016.12.040.
URL http://www.sciencedirect.com/science/article/pii/S0301421516307078

[8] J. L. Prol, K. W. Steininger, Photovoltaic self-consumption regulation in spain: Profitability analysis and alternative regulation schemes, Energy Policy 108 (2017) 742 – 754 (2017). doi:https://doi.org/10.1016/j.enpol.2017.06.019.
URL http://www.sciencedirect.com/science/article/pii/S0301421517303750

[9] C. Mateo, R. Cossent, T. Gómez, G. Prettico, P. Frías, G. Fulli, A. Meletiou, F. Postigo, Impact of solar pv self-consumption policies on distribution networks and regulatory implications, Solar Energy 176 (2018) 62 – 72 (2018). doi:https://doi.org/10.1016/j.solener.2018.10.015.
URL http://www.sciencedirect.com/science/article/pii/S0038092X18309940

[10] M. Londo, R. Matton, O. Usmani, M. van Klaveren, C. Tigchelaar, S. Brunsting, Alternatives for current net metering policy for solar pv in the netherlands: A comparison of impacts on business case and purchasing behaviour of private homeowners, and on governmental costs, Renewable Energy 147 (2020) 903 – 915 (2020). doi:https://doi.org/10.1016/j.renene.2019.09.062.
URL http://www.sciencedirect.com/science/article/pii/S0960148119313928

[11] E. Barbour, M. C. González, Projecting battery adoption in the prosumer era, Applied Energy 215 (2018) 356 – 370 (2018). doi:https://doi.org/10.1016/j.apenergy.2018.01.056.
URL http://www.sciencedirect.com/science/article/pii/S0306261918300618

[12] J. von Appen, M. Braun, Interdependencies between self-sufficiency preferences, techno-economic drivers for investment decisions and grid integration of residential pv storage systems, Applied Energy 229 (2018)

1140 – 1151 (2018). doi:https://doi.org/10.1016/j.apenergy.2018.08.003.
URL http://www.sciencedirect.com/science/article/pii/S0306261918311589

[13] K. Milis, H. Peremans, S. V. Passel, Steering the adoption of battery storage through electricity tariff design, Renewable and Sustainable Energy Reviews 98 (2018) 125 – 139 (2018). doi:https://doi.org/10.1016/j.rser.2018.09.005.

[14] Z. Ren, G. Grozev, A. Higgins, Modelling impact of pv battery systems on energy consumption and bill savings of australian houses under alternative tariff structures, Renewable Energy 89 (2016) 317 – 330 (2016). doi:https://doi.org/10.1016/j.renene.2015.12.021.
URL http://www.sciencedirect.com/science/article/pii/S0960148115305280

[15] C. B. Doménech, M. Heleno, Estimating the value of second life batteries for residential prosumers, in: 2019 IEEE Milan PowerTech, 2019, pp. 1–6 (June 2019).

[16] E. L. Ratnam, S. R. Weller, C. M. Kellett, Scheduling residential battery storage with solar pv: Assessing the benefits of net metering, Applied Energy 155 (2015) 881 – 891 (2015). doi:https://doi.org/10.1016/j.apenergy.2015.06.061.
URL http://www.sciencedirect.com/science/article/pii/S0306261915008193

[17] O. Talent, H. Du, Optimal sizing and energy scheduling of photovoltaic-battery systems under different tariff structures, Renewable Energy 129 (2018) 513 – 526 (2018). doi:https://doi.org/10.1016/j.renene.2018.06.016.
URL http://www.sciencedirect.com/science/article/pii/S0960148118306463

[18] G. Cardoso, M. Stadler, M. Bozchalui, R. Sharma, C. Marnay, A. Barbosa-Póvoa, P. Ferrão, Optimal investment and scheduling of distributed energy resources with uncertainty in electric vehicle driving schedules, Energy 64 (2014) 17 – 30 (2014).

[19] S. Mashayekh, M. Stadler, G. Cardoso, M. Heleno, A mixed integer linear programming approach for optimal der portfolio, sizing, and placement in multi-energy microgrids, Applied Energy 187 (2017) 154 – 168 (2017).

[20] Y. Yamamoto, Feed-in tariffs combined with capital subsidies for promoting the adoption of residential photovoltaic systems, Energy Policy 111 (2017) 312 – 320 (2017). doi:https://doi.org/10.1016/j.enpol.2017.09.041.

[21] I. Pérez-Arriaga, A. Bharatkuma, A framework for redesigning distribution network use of system charges under high penetration of distributed energy resources: new principles for new problems, Tech. rep., MIT CEEPR (2014).

[22] M. Chesser, J. Hanly, D. Cassells, N. Apergis, The positive feedback cycle in the electricity market: Residential solar pv adoption, electricity demand and prices, Energy Policy 122 (2018) 36 – 44 (2018).

[23] D. W. Cai, S. Adlakha, S. H. Low, P. D. Martini, K. M. Chandy, Impact of residential pv adoption on retail electricity rates, Energy Policy 62 (2013) 830 – 843 (2013). doi:https://doi.org/10.1016/j.enpol.2013.07.009.

[24] R. Boero, S. N. Backhaus, B. K. Edwards, The microeconomics of residential photovoltaics: Tariffs, network operation and maintenance, and ancillary services in distribution-level electricity markets, Solar Energy 140 (2016) 188 – 198 (2016). doi:https://doi.org/10.1016/j.solener.2016.11.010.
URL http://www.sciencedirect.com/science/article/pii/S0038092X16305266

[25] R. Tonkoski, D. Turcotte, T. H. M. EL-Fouly, Impact of high pv penetration on voltage profiles in residential neighborhoods, IEEE Transactions on Sustainable Energy 3 (3) (2012) 518–527 (2012).

[26] P. Chen, R. Salcedo, Q. Zhu, F. de Leon, D. Czarkowski, Z. Jiang, V. Spitsa, Z. Zabar, R. E. Uosef, Analysis of voltage profile problems due to the penetration of distributed generation in low-voltage secondary distribution networks, IEEE Transactions on Power Delivery 27 (4) (2012) 2020–2028 (Oct 2012).

[27] G. E. Constante-Flores, M. S. Illindala, Data-driven probabilistic power flow analysis for a distribution system with renewable energy sources using monte carlo simulation, IEEE Transactions on Industry Applications 55 (1) (2019) 174–181 (Jan 2019). doi:10.1109/TIA.2018.2867332.

[28] M. Nijhuis, M. Gibescu, S. Cobben, Gaussian mixture based probabilistic load flow for lv-network planning, IEEE Transactions on Power Systems 32 (4) (2017) 2878–2886 (July 2017). doi:10.1109/TPWRS.2016.2628959.

[29] C. Carmona-Delgado, E. Romero-Ramos, J. Riquelme-Santos, Probabilistic load flow with versatile non-gaussian power injections, Electric Power Systems Research 119 (2015) 266 – 277 (2015). doi:https://doi.org/10.1016/j.epsr.2014.10.006.
URL http://www.sciencedirect.com/science/article/pii/S0378779614003605

[30] T. Power, G. Verbic, A. C. Chapman, A nonparametric bayesian methodology for synthesizing residential solar generation and demand data, IEEE Transactions on Smart Grid (2019) 1–1 (2019). doi:10.1109/TSG.2019.2956785.

[31] M. Kabir, Y. Mishra, R. Bansal, Probabilistic load flow for distribution systems with uncertain pv generation, Applied Energy 163 (2016) 343 – 351 (2016). doi:https://doi.org/10.1016/j.apenergy.2015.11.003.
URL http://www.sciencedirect.com/science/article/pii/S0306261915014440

[32] P. S. Georgilakis, N. D. Hatziargyriou, A review of power distribution planning in the modern power systems era: Models, methods and future research, Electric Power Systems Research 121 (2015) 89 –

100 (2015). doi:https://doi.org/10.1016/j.epsr.2014.12.010.
URL http://www.sciencedirect.com/science/article/pii/S0378779614004490

[33] A. Sani Hassan, L. Cipcigan, N. Jenkins, Optimal battery storage operation for pv systems with tariff incentives, Applied Energy 203 (2017) 422 – 441 (2017). doi:https://doi.org/10.1016/j.apenergy.2017.06.043.
URL http://www.sciencedirect.com/science/article/pii/S030626191730778X

[34] A. Sani Hassan, L. Cipcigan, N. Jenkins, Impact of optimised distributed energy resources on local grid constraints, Energy 142 (2018) 878 – 895 (2018). doi:https://doi.org/10.1016/j.energy.2017.10.074.
URL http://www.sciencedirect.com/science/article/pii/S0360544217317796

[35] A. Maheshwari, M. Heleno, M. Ludkovski, The effect of rate design on power distribution reliability considering adoption of distributed energy resources, Applied Energy 268 (2020) 114964 (2020). doi:https://doi.org/10.1016/j.apenergy.2020.114964.

[36] S. Candas, K. Siala, T. Hamacher, Sociodynamic modeling of small-scale pv adoption and insights on future expansion without feed-in tariffs, Energy Policy 125 (2019) 521 – 536 (2019).

[37] C. Thormeyer, J.-P. Sasse, E. Trutnevyte, Spatially-explicit models should consider real-world diffusion of renewable electricity: Solar pv example in switzerland, Renewable Energy 145 (2020) 363 – 374 (2020). doi:https://doi.org/10.1016/j.renene.2019.06.017.
URL http://www.sciencedirect.com/science/article/pii/S0960148119308390

[38] F. Heymann, V. Miranda, F. J. Soares, P. Duenas, I. P. Arriaga, R. Prata, Orchestrating incentive designs to reduce adverse system-level effects of large-scale ev/pv adoption – the case of portugal, Applied Energy 256 (2019) 113931 (2019). doi:https://doi.org/10.1016/j.apenergy.2019.113931.
URL http://www.sciencedirect.com/science/article/pii/S0306261919316186

[39] M. Deru et al., U.S. Department of Energy Commercial Reference Building Models of the National Building Stock, Tech. rep., NREL (February 2011).

[40] S. T. Anderson, R. G. Newell, Information programs for technology adoption: the case of energy-efficiency audits, Resource and Energy Economics 26 (1) (2004) 27–50 (2004).

[41] A. M. Leite da Silva, A. M. de Castro, Risk assessment in probabilistic load flow via monte carlo simulation and cross-entropy method, IEEE Transactions on Power Systems 34 (2) (2019) 1193–1202 (2019).

[42] H. Wu, Y. Zhou, S. Dong, Y. Song, Probabilistic load flow based on generalized polynomial chaos, IEEE Transactions on Power Systems 32 (1) (2017) 820–821 (2017).

[43] D. Zhang, Z. Fu, L. Zhang, An improved ts algorithm for loss-minimum reconfiguration in large-scale distribution systems, Electric Power Systems Research 77 (5) (2007) 685 – 694 (2007). doi:https://doi.org/10.1016/j.epsr.2006.06.005.
URL http://www.sciencedirect.com/science/article/pii/S0378779606001477

[44] S. Wilcox, W. Marion, Users Manual for TMY3 Data Sets, Tech. rep., NREL (May 2008).